We are IntechOpen,
the world's leading publisher of
Open Access books
Built by scientists, for scientists

6,900
Open access books available

186,000
International authors and editors

200M
Downloads

Our authors are among the

154
Countries delivered to

TOP 1%
most cited scientists

12.2%
Contributors from top 500 universities

CLARIVATE ANALYTICS
BOOK CITATION INDEX
INDEXED

WEB OF SCIENCE™

Selection of our books indexed in the Book Citation Index
in Web of Science™ Core Collection (BKCI)

Interested in publishing with us?
Contact book.department@intechopen.com

Numbers displayed above are based on latest data collected.
For more information visit www.intechopen.com

Wind Turbines Integration with Storage Devices: Modelling and Control Strategies

Samuele Grillo[1], Mattia Marinelli[2] and Federico Silvestro[2]
[1]Dipartimento di Elettrotecnica – Politecnico di Milano
[2]Dipartimento di Ingegneria Navale ed Elettrica – Università di Genova
Italy

1. Introduction

The electric power system is facing an evolution from the traditional concept of energy generation by few localized power plants interconnected to a meshed system to distributed medium and small scale generators (Thomas, 2009; Neural et al. 2008).

Moreover some typologies of these generators embedded into the distribution network are fed by renewable sources like wind and sunlight. Their main drawback is their hardly predictable behaviour and uncontrollable output. This means having for example maximum production during minimum demand period or excess of generation in congested parts of the electric network, thus causing bottlenecks and overvoltage situations in some critical sections of the grid (Grillo et al., 2009).

The presence of energy storage systems may allow a better management of the electric system allowing the full exploitation of renewable energy sources. Nowadays the cost per stored energy is quite high and so it might not be economically feasible to install huge amount of batteries. The size of the storage systems can considerably vary and, depending on their sizes, different tasks can be performed as shown in Fig1 (Fioravanti et al., 2009).
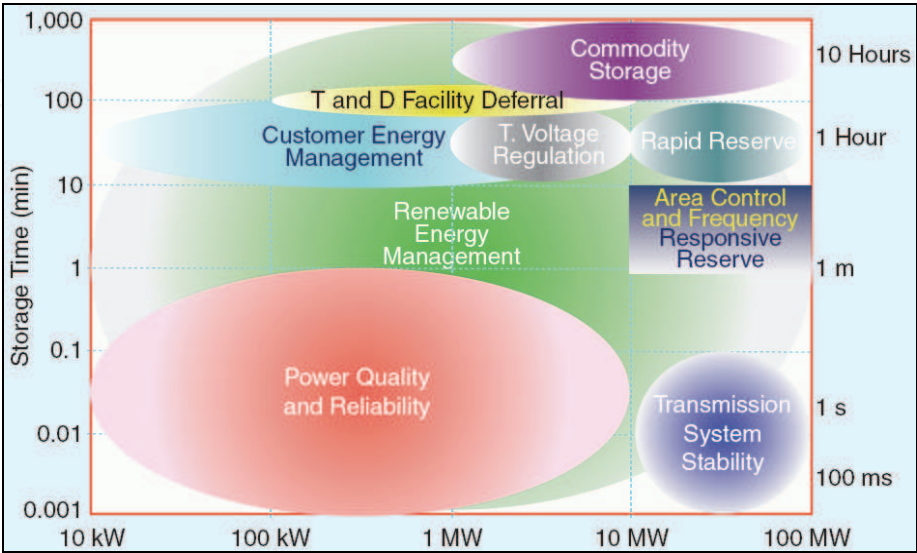

Fig. 1. Storage power requirements for electric power utility applications

Hence the possible duties range from short-term fluctuation levelling and power quality improvement to primary frequency-power regulation and, in case of large storage sizing, compliance to day-ahead generation dispatching (Oudalov et al., 2005).

The present work focuses on the development of models of wind turbines and storage systems, in Matlab-Simulink environment, for implementing integrated control strategies of the whole resulting system in order to describe the benefits that storage can provide. Hence, the idea is to control the battery charging and discharging phases in order to control the whole plant output.

The wind park is composed by four 2 MW wind turbines and a storage system of 2 MWh – 2.5 MW equipped with Na-NiCl$_2$ batteries. Both the wind turbine and the storage models have general validity and are suited for electrical studies (Di Rosa et al., 2010).

The chapter is organized as follows:

- Paragraph 2 describes the model of the wind turbine and analyzes the wind speed profiles used in the study;
- Paragraph 3 illustrates the storage model;
- Paragraph 4 analyzes the layout of the plant system and the control strategy implemented;
- Paragraph 5 describes the result of the simulations performed.
- Paragraph 6 reports the conclusion and the further developments.

2. Wind turbine model

2.1 Main assumptions

The wind turbine model is described from an electromechanical perspective, thus it provides: an analysis of the aerodynamic behaviour of the rotor including the pitch control system, the shaft dynamic and the maximum power tracking characteristic (Ackermann et al., 2005; Marinelli et al., 2009).

The wind turbine model is tuned for a 2 MW full converter direct drive equipped generator. This typology of wind turbine is characterized by the absence of the gearbox and the presence of ac/dc/ac converter sized for the whole power, as depicted in Fig. 2.
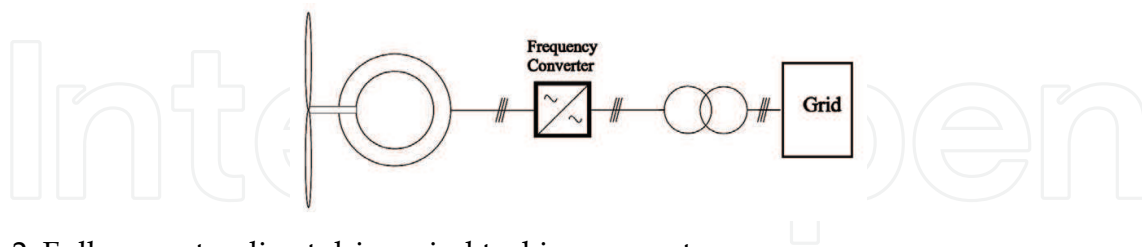

Fig. 2. Full converter direct drive wind turbine concept

Since the model is not intended to analyze dynamics faster than a fraction of second, there is no need to characterize in a detailed way the generation/conversion system, which thus it is modelled as a negative load (Achilles & Pöller, 2004). The rest of the electromechanical conversion system needs an accurate detail due to the interest in studying the possibility to reduce the output in certain conditions. There is, in fact, the need to model the delays introduced by the pitch controller and by the shaft rotational speed.

The block diagram that describes the main model components and their mutual interaction is depicted in Fig. 3. Reading the picture from left to right the first block met is the

aerodynamic one that evaluates the power harvested by the rotor that depends on wind speed, rotational speed and blade angle. This accelerating power, along with the rotational speed of the generator, enters the block that describes the shaft behaviour and allows the evaluation of the power at the end of the shaft and of the turbine rotational speed. The accelerating power at the end of the shaft is the input for the block called generator and MPT (Maximum Power Tracking) that describes the dynamic of the generator and of the MPT control characteristic, as well as the efficiency of the conversion system. At the end the electrical power produced is calculated and is the main output of the turbine model.
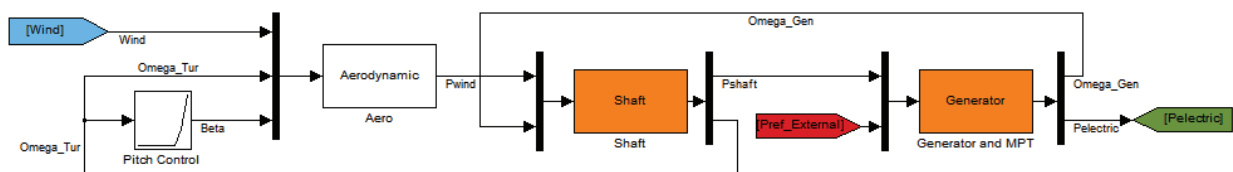

Fig. 3. Conceptual block diagram of the wind turbine

The paragraph develops as follow:
- Wind speed data analysis
- Rotor aerodynamic
- Shaft dynamic
- MPT characteristic
- Pitch controller

2.2 Wind speed data

When studying the wind turbine output, special care should be devoted to the analysis and the proper use of the wind speed data. For power system studies it is common practice to consider just one wind profile per turbine while, in reality, during their sweeping action the blades face different wind profiles: this variety is generated by the turbulence induced by the local terrain. This assumption however is commonly accepted as long as this wind is representative of the wind seen by the whole rotor and it is generally called hub wind (Sørensen et al., 2001).

Due to the interest in studying the fluctuation induced in the turbine power output it is necessary to have appropriated wind speed data or an accurate wind model. For this purpose, data related to the power outputs and to the wind speeds measured at the nacelle of 4 wind turbines belonging to the same farm are used. The data are sampled with a five seconds time step that gives accurate information on the fluctuation included in the wind. A comparison between the wind speeds, measured by the anemometer placed in the rear of the nacelle, and the electrical output power highlights that the wind measured by the anemometer is not necessary the same that is seen by the whole rotor. As shown in Fig. 4 it can be seen that there is a tight correlation between the wind measured data and power output. This correlation determines the datasheet power curve of the turbine, although being this correspondence not exact.

Due to this weak correlation, it is chosen to evaluate the wind speed starting from the output power profile by means of the static power curve of the turbine. Moreover the reduction in the power output due to the height of the installation of the farm, caused by the lower atmospheric pressure compared to sea level, is taken in account. The wind series thus
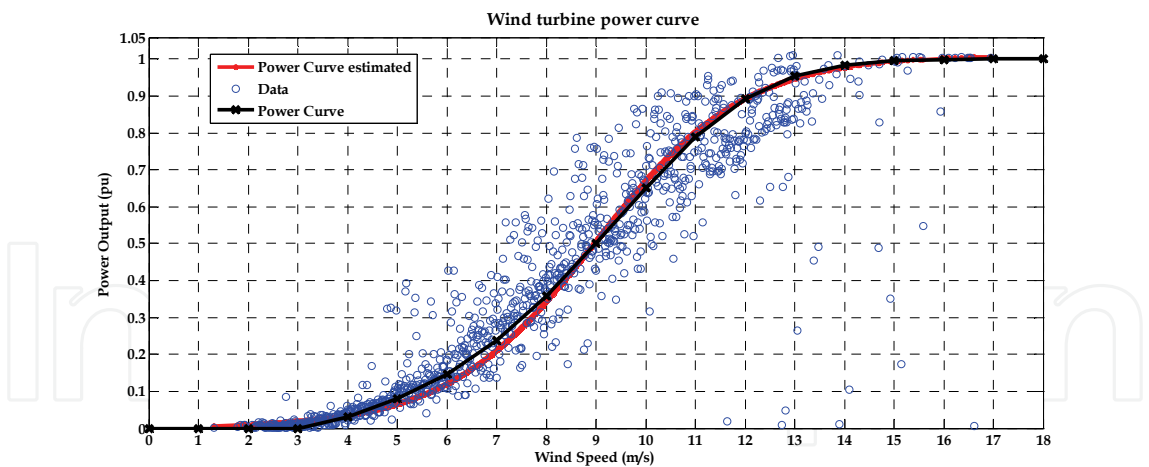
Fig. 4. Datasheet power curve (black curve) and curve estimated from the data (red curve)

created contain information related to the turbulence due to the local terrain roughness or others as for example the tower shadow effect or the wake of the surrounding machines.
Fig. 5 offers a visual comparison between two 12-hours series of wind speed: the one on the left side reports the wind measured at the nacelle, while the one on the right side shows the wind calculated from the power production.
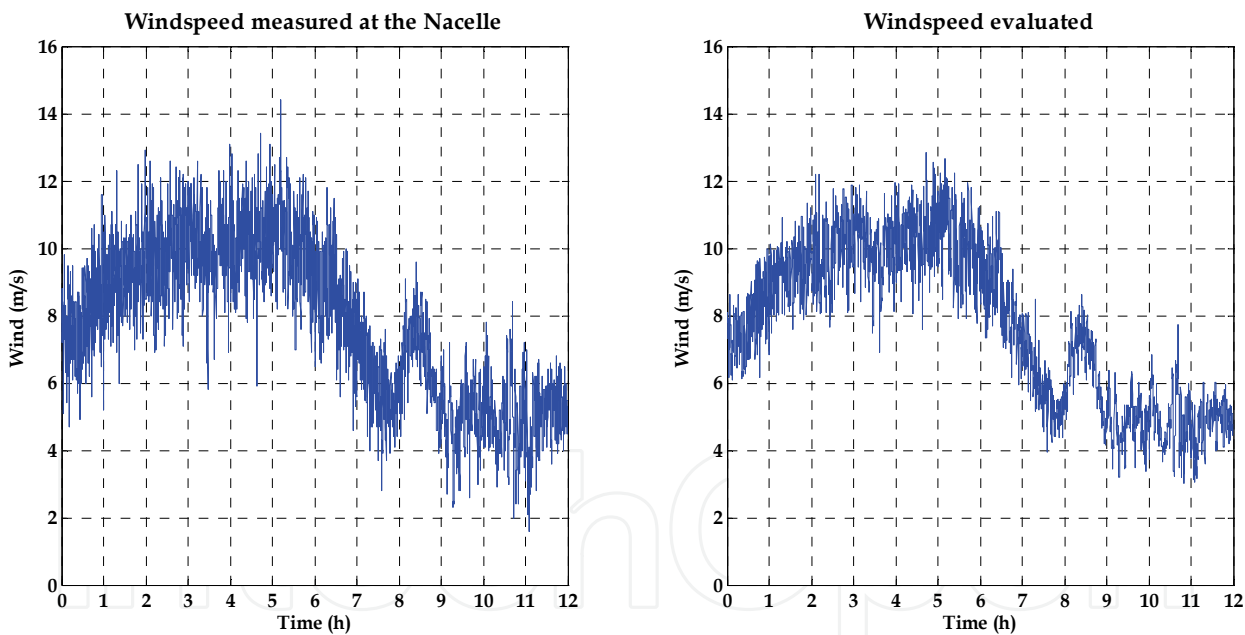

Fig. 5. 12-hours length wind speed profiles, 5-seconds sampled, measured by the nacelle anemometer (left picture) and deduced from the power output (right picture)

As it can be noticed the wind calculated is smoother because the wind measured by the nacelle anemometer has the turbulence induced by the blades themselves.
To analytically evaluate the turbulence it is common practice to introduce the turbulence intensity, generally defined as the ratio between the standard deviation and the average wind speed in a 10-minutes length wind series. In the specific case the average turbulence intensity on all the 12-hours profile, calculated as the average of all the 10-minutes measures, values 12% for the wind series measured at the nacelle and 9% for the one

evaluated from the power output. Fig. 6 shows the two 10-minutes average wind speeds and the related turbulence intensity profiles.
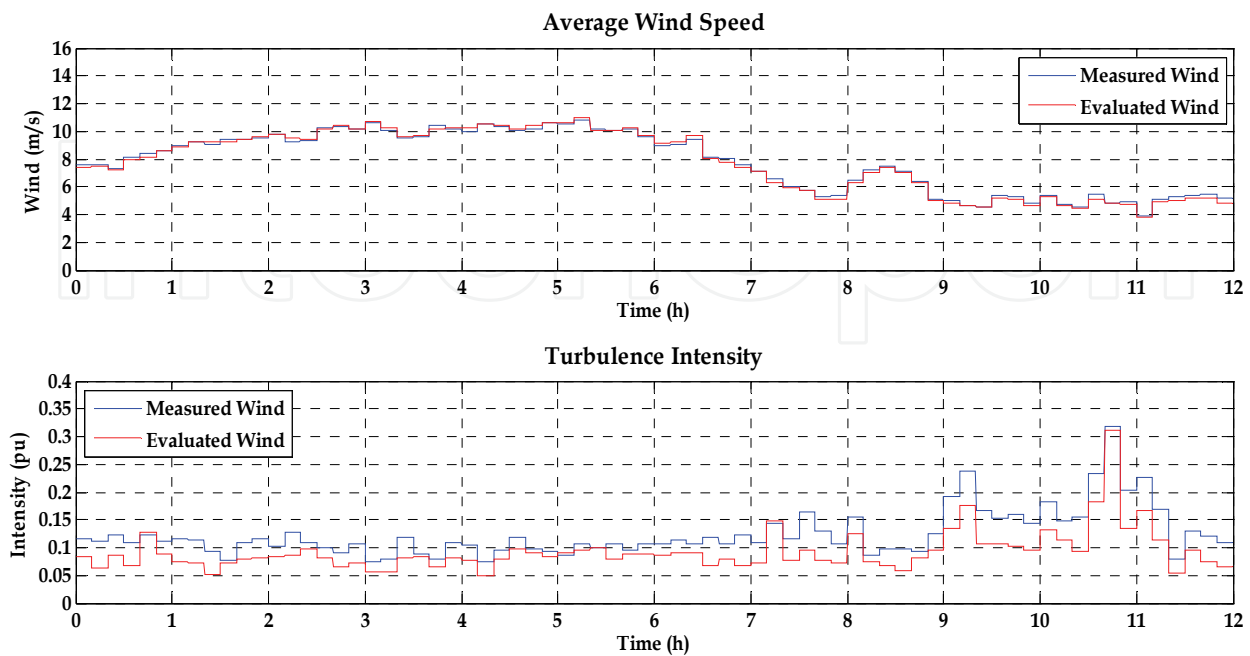

Fig. 6. Measured and Evaluated winds: 10-minutes average (first diagram) and turbulence intensity (second diagram)

In addition, the four turbines are fed by different wind speeds profiles calculated, as explain previously, from the power output of four wind turbines belonging to the same wind farm. Fig. 7 shows a window of 2-hours in order to better appreciate the correlation between the four series.
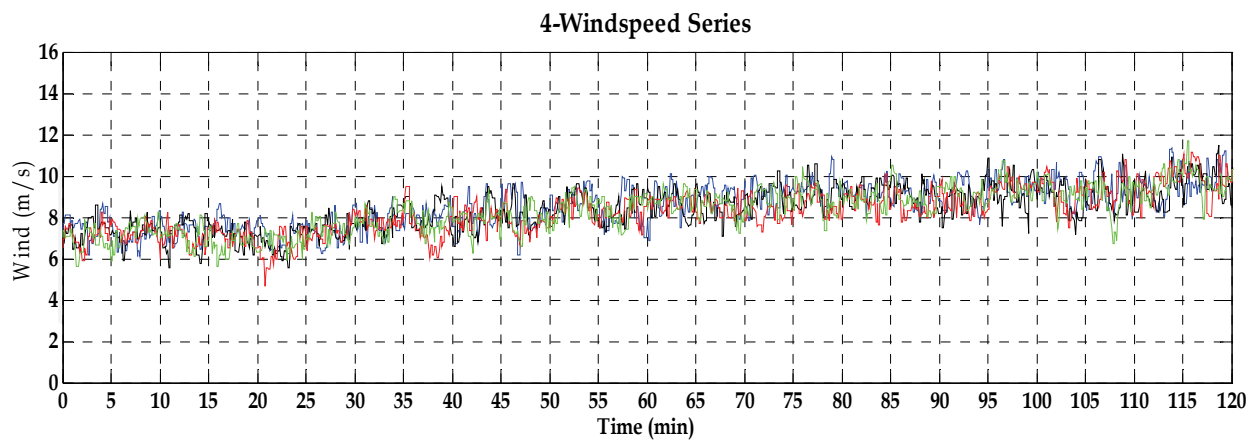

Fig. 7. Four wind speed profiles, 5-seconds sample time, 2-hours timeframe.

2.3 Aerodynamic

The power that the rotor of area, A (m^2), can extract from the wind flux depends mainly on the wind speed, U (m/s), the air density, ρ (kg/m^3), and rotor aerodynamic efficiency, c_p (pu), which is also known as power coefficient and quantifies the rate of power that the rotor extracts from the wind, P_{rotor} (W):

$$P_{rotor} = \frac{1}{2} c_p \cdot \rho \cdot A \cdot U^3 \qquad (1)$$

This coefficient is function of the Tip Speed Ratio, λ (pu), and of the blade pitch angle, β (deg). The value of λ depends on the ratio between blade peripheral speed and wind speed.

$$\lambda = \omega \cdot R / U \qquad (2)$$

A possible analytic representation can be expressed by the following equation:

$$c_p = c_1 * \left\{ c_6 * \lambda + \frac{\left[-c_4 - c_3 * (2,5+\beta) + c_2 * \dfrac{1}{\lambda + c_7 * (2,5+\beta)} - \dfrac{c_8}{\lambda + (2,5+\beta)^3} \right]}{\exp[c_5 * (\dfrac{1}{\lambda + c_7 * (2,5+\beta)} - \dfrac{c_8}{\lambda + (2,5+\beta)^3})]} \right\} + c_9 * \lambda \qquad (3)$$

where the coefficients c_i are:

c_1	c_2	c_3	c_4	c_5	c_6	c_7	c_8	c_9
0,645	116	0,4	5	21	0,00912	0,08	0,035	0,001

Table 1. Coefficient values

The graphical representation of the power coefficient curves in function of the tip speed ratio and parameterized at different pitch angle values is depicted in Fig. 8
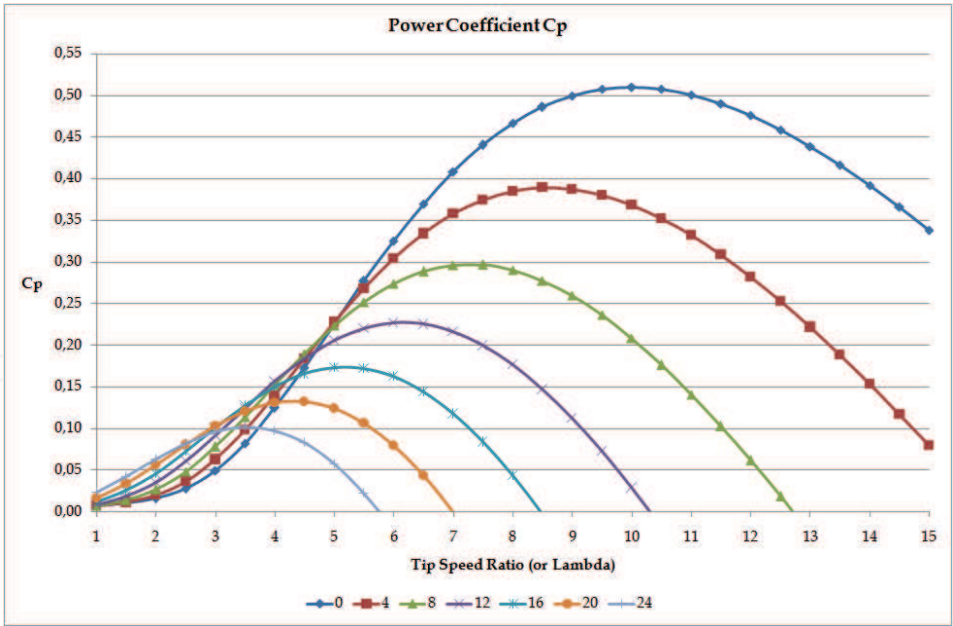

Fig. 8. Power Coefficient characteristic plotted in function of the Tip Speed Ratio (lambda) and parameterized with the pitch angle (beta).

2.4 Shaft

Wind turbines have a relatively soft shaft, and the eigenvalues of the drive train are inside the range of values normally taken in account for power system studies (0.1 ÷ 10 Hz).

Moreover the greater is the number of pole pairs of the generator the softer gets the shaft (Akhmatov, 2003). This can cause the initiation of oscillations whenever there is a sudden step of torque, due for example to wind gust or faults on the network.

In fact, whenever there is a sudden difference between mechanical and electrical torques, respectively T_{wind} and $T_{electromagnetic}$ (Nm), the two shafts, the one of the turbine and the one of the generator, have the possibility to rotate one against the other, thus there is the need to define two different rotational speeds: $\omega_{turbine}$ and $\omega_{generator}$ (rad/s). A two masses representation is therefore necessary due to the interest in evaluating the oscillations induced by the wind in power output. The differential equations that describe the dynamic of the system are reported below: starting from the response determined by the inertia of the turbine, $J_{turbine}$ (kg m²), passing through the shaft stiffness, k (Nm/rad), and damping, D (Ns/rad), values getting to the generator inertia, $J_{generator}$:

$$\begin{cases} T_{wind} - T_{shaft} = J_{tur} * \dfrac{d\omega_{tur}}{dt}; \\ \omega_{turbine0} = \omega_{initial} \end{cases} \quad (4)$$

$$\begin{cases} T_{shaft} = k * \vartheta + D * (\omega_{turbine} - \omega_{generator}); \\ \vartheta = \int (\omega_{turbine} - \omega_{generator}) * dt; \\ \vartheta_0 = {T_{shaft0}}\big/{k} \end{cases} \quad (5)$$

$$\begin{cases} T_{shaft} - T_{electromagnetic} = J_{gen} * \dfrac{d\omega_{gen}}{dt}; \\ \omega_{generator0} = \omega_{initial} \end{cases} \quad (6)$$

In order to help the comprehension of the shaft dynamics, a comparison with the electrical equivalent system can be done. In fact, if it is assumed that the torques behave like the currents and the rotational speeds like the voltages then the inertial effects are described by means of capacitors, the stiffness by means of inductor and the damping by means of resistance. The electrical circuit is shown in Fig. 9.
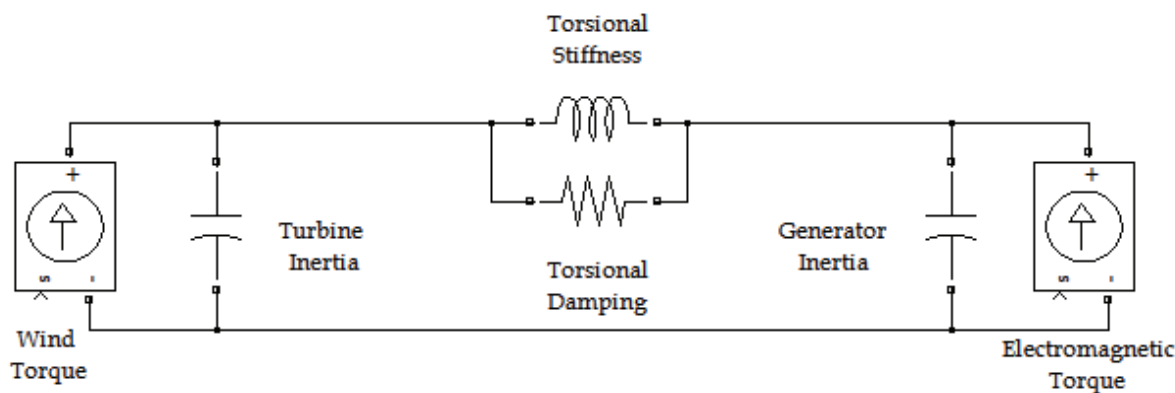

Fig. 9. Electrical equivalent of the two masses shaft.

2.5 Maximum power tracking characteristic

As already described in the aerodynamic characteristic, the maximum efficiency is available only for a small range of values of λ. Thus, since the wind is continuously changing, the Maximum Power Tracking (MPT) has to control the generator rotational speed, ω, in order to have the desired (and optimal) power output. This tracking action is realized by following the curve, shown in Fig. 10., which generates the reference power in function of the rotational speed of the turbine.

In theory it would be better to express the reference power as function of the wind speed, which, unfortunately, cannot be measured with accuracy. So, instead of using wind speed, another control variable, the rotational speed of the turbine is used (Hansen et al., 2007).

The logic behind this curve is quite simple: the control system sets a reference value of power to the generator, depending on the actual rotational speed, and, if the torque that the generator imposes on the shaft is greater than the one caught by the rotor blades, then the shaft slows down. Hence the reference power is reduced and if it is equal to the one produced by the turbine the system is steady otherwise the tracking action goes on.
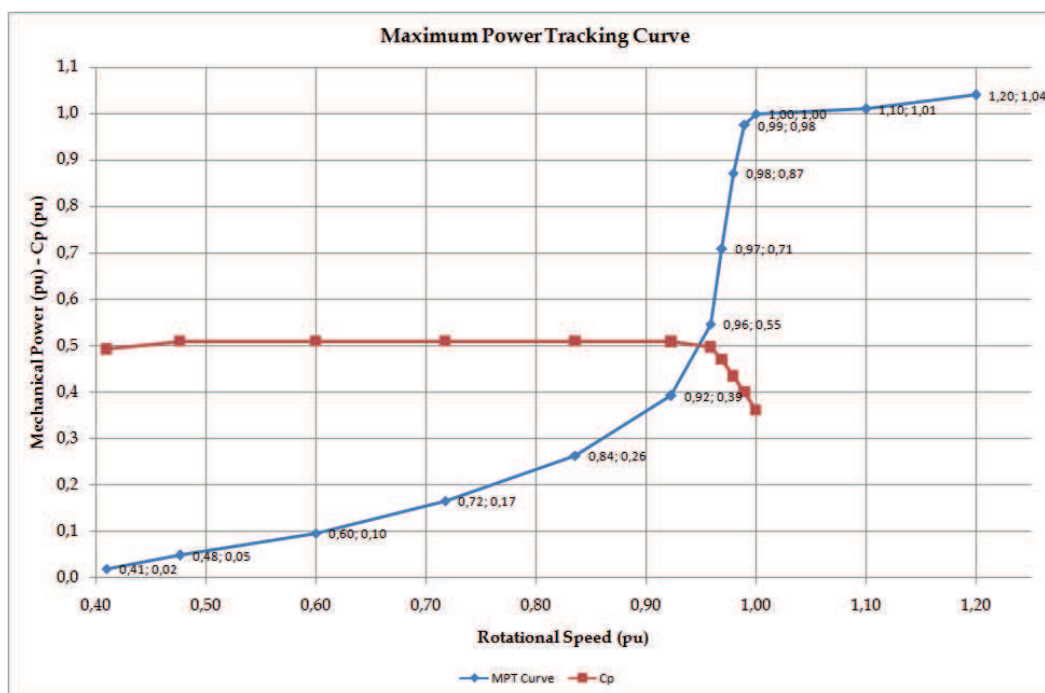

Fig. 10. Power reference (MPT characteristic) and c_p in function of the rotational speed.

This curve can be divided into three zones:

- the first one goes from the cut-in rotational speed (40% of the nominal speed) to the 90% and describes the part where the turbine is pursuing the maximum power coefficient (depicted by the red curve) and covers the wind range between 3 to 9 m/s.
- the second zone is characterized by the steep increase in the reference power and it is due to the fact that there is no more interest in collecting all the power in the wind because it is blowing close to the nominal values. Thus the power coefficient is progressively reduced. It includes the winds between 9 and the nominal one, which is equal to 12.5 m/s for the modelled turbine.
- the last one is characterized by a flat curve that sets the nominal reference power to the generators and allows the machine to go in overspeed to absorb the rapid wind speed

variations. Generally a 20% of overspeed is acceptable and a slight increase of the power output (about 4%) can help to reduce the stress on the pitch blade actuators. The wind speed covered by this area obviously ranges from the nominal wind speed to the cut-out one (25 m/s).

The c_p curve is no more represented since from there the blade angle can assume different transient values from 0° (optimal angle) to 32° and hence it is not possible to define a unique value power coefficient value.

Fig. 11 reports the influence of the reference power set by the MPT curve in the modeling block diagram. As it can be seen this reference power value can be modified by an external control signal that reduces the reference power in order to force a reduction in the turbine power output in case of request by the overall park controller. This reduction in the electromagnetic torque (the braking one) will cause an acceleration of the turbine speed that will be duty of the pitch control system to counteract.
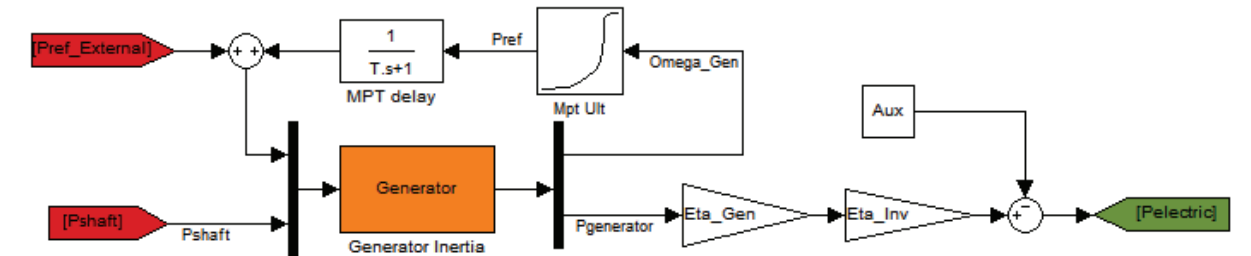

Fig. 11. MPT and generator block diagram.

2.6 Pitch angle control

The pitch control system has to reduce the aerodynamic efficiency by increasing the blade attack angle. Its control is sensible to rotational speed: if this value goes above 1 per unit, the PI (proportional-integral) control system commands the increase of the blade pitch angle. Fig. 12 shows the block diagram of the pitch control system that includes also the delay of the actuator that is realized by the integrator with unitary feedback (on the right side of the figure).
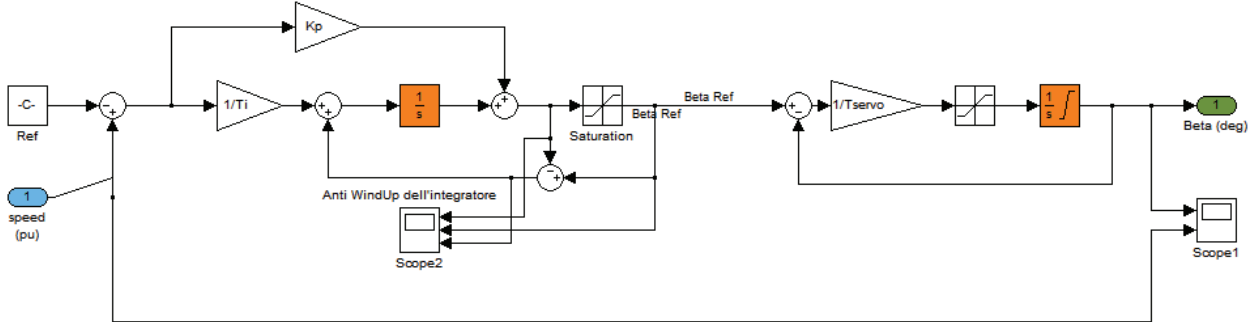

Fig. 12. Block diagram of the pitch controller.

3. Storage model

3.1 Main assumptions

The storage model proposed is suited for electrical studies and it has a general validity (Chen & Rincon Mora, 2006). The model has a nominal power of 2.5 MW and a nominal

energy of 2 MWh, it is composed by a set of 140 units, each with nominal values of 17.8 kW – 14.2 kWh; each unit is composed by 2 parallels of 108 cells connected in series. It is assumed that all the cells are perfectly balanced and thus the tasks requested to the storage system are equally divided among the 140 units. Under this assumption all the dynamics are built in the single equivalent cell; the overall storage desired size is then obtained by multiplying/dividing the cell parameters for the number of series/parallel elements.

The modelled dynamics regard the State-of-Charge (SOC) behaviour, the electrochemical conversion and the thermal characterization. The main state variables are therefore the state of charge and the temperature: all the characteristic elements of the storage system (as open circuit voltage, internal resistance and protection thresholds) present some kind of dependence from these state variables. Therefore the relationships among them are highlighted further on. An overview of the electrical equivalent of the abovementioned dynamics of the equivalent cell is proposed in Fig. 13.
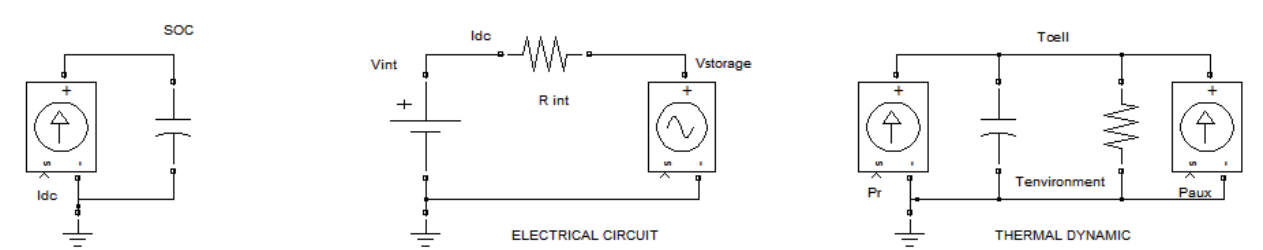

Fig. 13. Electrical equivalent of the main dynamics analysed for the description of the storage system.

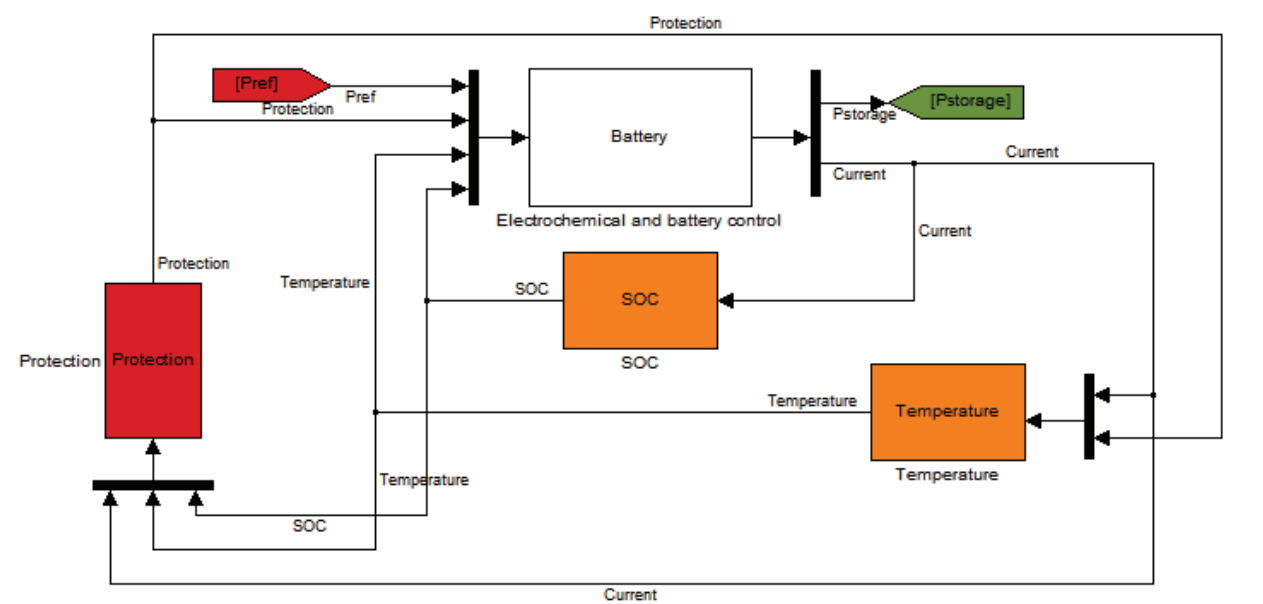The relationships of these dynamics are depicted in the conceptual block diagram shown in Fig. 14.

Fig. 14. Conceptual block diagram of the battery model.

The cell electrochemical conversion relations and the current controller are included in the block named Battery. The input values are the desired power that the battery must produce (or absorb, if negative), the protection signal that blocks the battery due to low or high state

of charge or temperature, the values of the SOC and of the temperature, which are needed to evaluate specific cell parameters such as the Open Circuit Voltage and the internal resistance. The output is of course the effectively produced power as well as the current flowing in the cells necessary to describe the behaviour of the SOC and the increase in the internal temperature due to Joule losses.

The paragraph develops as follow:

- State-Of-Charge
- Electrochemical dynamic
- Current control loop
- Thermal dynamic
- Protections and limitations

3.2 State-Of-Charge

The first dynamic described is related to the behaviour of the state of charge (SOC). This variable gives information about the quantity of energy still stored in the battery.

Its value is 1 when the battery is fully charged and 0 when fully discharged. Because of the nature of Na-NiCl$_2$ it is not recommended to discharge it below 0.2. The differential equation is shown further on: I_{dc} (A) is the current flowing in the battery and used by the auxiliary system; C is the nominal charge capacity, in Coulomb or Ah, of the battery.

$$\begin{cases} I_{dc} = C * \dfrac{dSOC}{dt} \\ SOC(0) = SOC_0 \end{cases} \tag{7}$$

The Na-NiCl$_2$ battery hasn't auto-discharge, so no shunt/dissipative elements are considered. In case of need to model the self discharge the previous equation is modified by the introduction of a resistive element, R, as follows:

$$\begin{cases} I_{dc} = \dfrac{SOC}{R} + C * \dfrac{dSOC}{dt} \\ SOC(0) = SOC_0 \end{cases} \tag{8}$$

3.3 Electrochemical dynamic

To evaluate the amount of energy that is stored or released by the battery the electrochemical dynamic has to be detailed. A first order model takes into account two voltage generators with a resistor in series as shown in Fig. 15. The first one, V_{oc}, generates what is commonly known as open circuit voltage and its nominal value is, for the Na-NiCl$_2$,
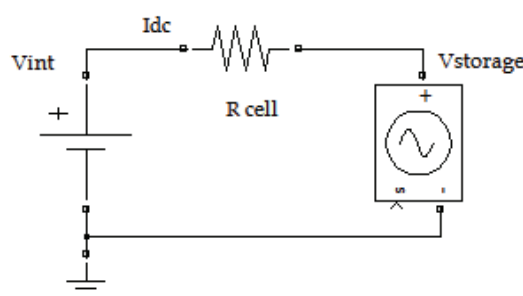

Fig. 15. Electrochemical equivalent.

2.58 Volt per cell, with a slight dependence on the SOC. The resistor takes into account the internal Joule losses and is assumed to be function of SOC and temperature.

The controlled generator, V_{batt}, models the behaviour of the dc/ac converter. Its task is to close the circuit and set, by the means of the control system, the current value to have the desired value of power flowing in the circuit. The current is assumed positive if it flows from V_{oc} to V_{batt} implying, hence, a discharge action.

The value of V_{oc} depends on the SOC as depicted by the characteristic (reported in physical values and per unit on a 2.58 V base) shown in Fig. 16 (Bossi et al, 2005).
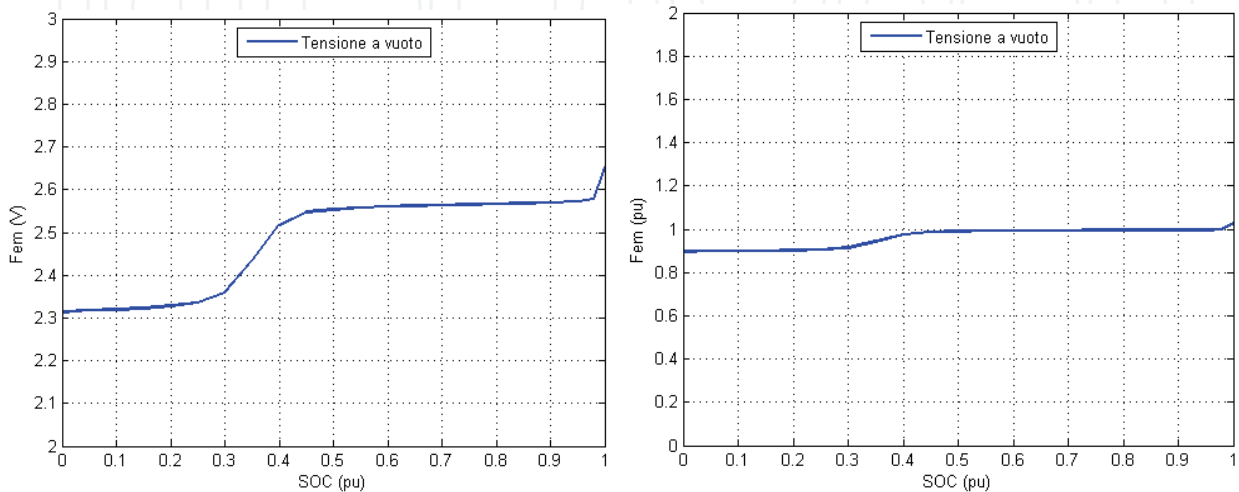

Fig. 16. Open cell voltage characteristic in function of the SOC in physical value (left picture) and per unit (right picture).

The behaviour of the internal cell resistance is displayed in Fig. 17.
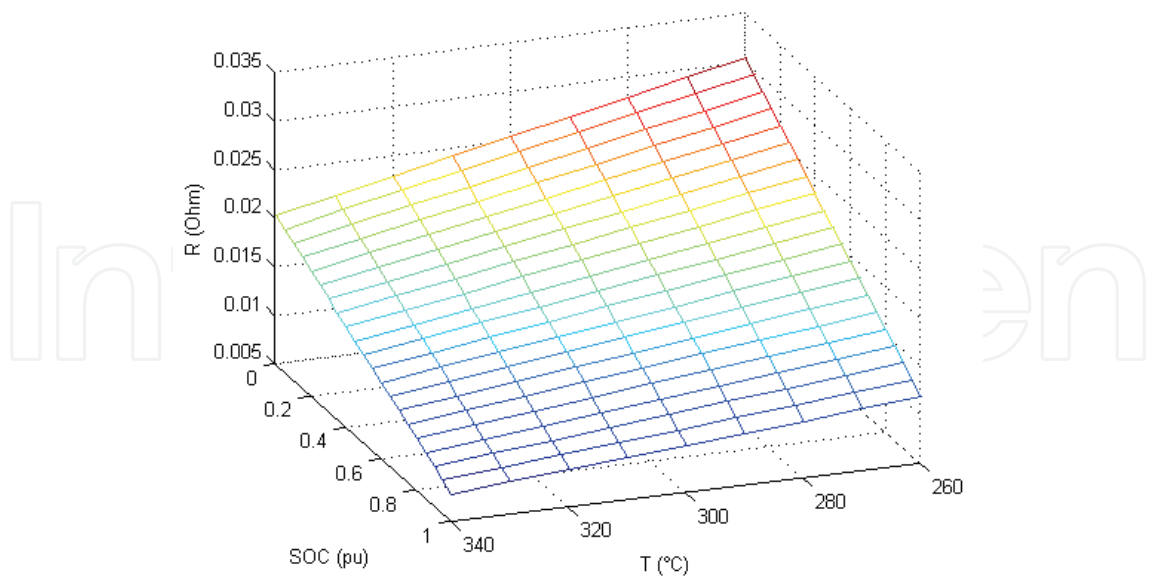

Fig. 17. Na-NiCl$_2$ cell internal resistance in function of SOC and temperature

The dependance of the resistance is not linear on the temperature and on the SOC. It can be noticed that the resistance increases with the decrease of the temperaure, this fact must kept in mind when setting the temperature thresholds that trigger the cooling fan.

3.4 Current control loop

The control of the power output is demanded to the current control loop. The power reference is converted in a current reference by the knowledge of the voltage at the connection point of the battery. The reference current is therefore compared with the current flowing in the battery system and the difference, the error, is the input for the PI (Proportional-Integral) controller. The output of the controller sets the values for the voltage source, that models the electronic converter; therefore the current flowing in the battery cells is evaluated by comparing this voltage with the open circuit voltage of the battery and by knowning the internal resistance. The integral action of the controller grants that the current error is zero in the steady state conditions. Fig. 18 summarizes graphically what above mentioned.
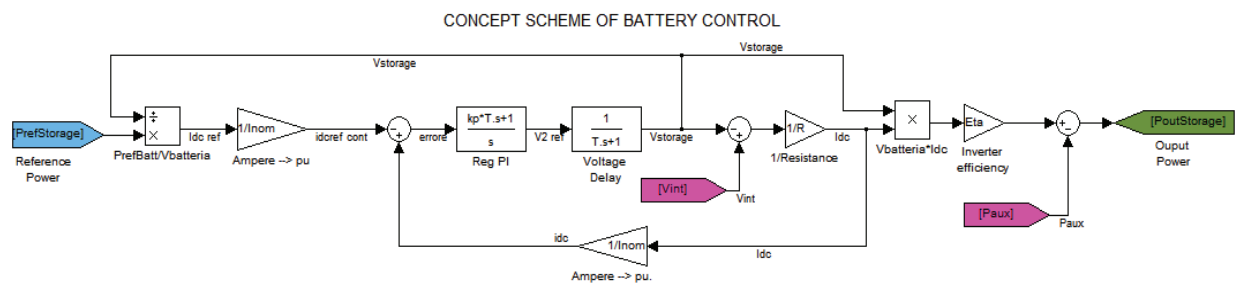

Fig. 18. Block diagram of the battery control.

3.5 Thermal dynamic

The thermal dynamic is very crucial when high power stress is required—this kind of management requires high currents leading to high thermal dissipation on internal resistance—and, moreover, for hot-temperature battery devices because they require working in a specific temperature range (e.g. 260 °C ÷ 360 °C for a Ni-NaCl$_2$ chemistry based battery). The battery model is equipped with auxiliary systems (fans and heaters) in order to enable the control system to keep temperature within the allowed range.

A possible representation is reported in Fig. 19. Using the electric components, the differential equations, reported subsequently, can be easily understood.
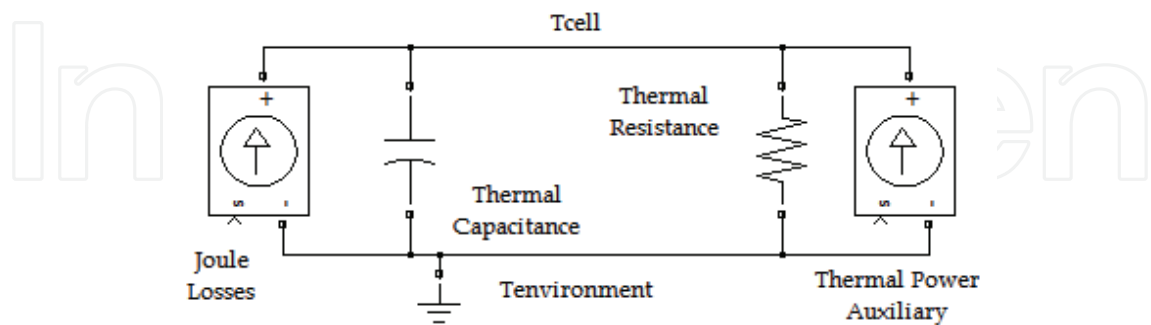

Fig. 19. Thermal dynamic described by the mean of electric equivalent.

If it is assumed that the temperature, T (°C), behaves like the voltage and the thermal power, Q (W), like the current, then the capacitor and the resistor represents the thermal capacitance, C_T (J/K), and the thermal resistance, R_T (K/W), of the battery. The two current generators are used to model the thermal power generated by Joule effect, Q_{Pr}, and the thermal contribution of both cooling fan and heater devices, Q_{Paux}.

$$\begin{cases} Q_{Pr} + Q_{Paux} + Q_R = Q_C \\ Q_R = {\Delta T}/{R_T} \\ Q_C = C_T * {dT}/{dt} \\ T(0) = T_0 \end{cases} \qquad (9)$$

3.6 Protection and limitation

The battery control system has the task to stop the battery if the SOC level approaches 0.2 or 1. It is also sensible to the temperature and for example it has to turn on the cooling fan when temperature goes above a threshold, that is function of SOC, or turn on heater devices if the battery is cooling down. The protection actions are summarized in Table 2.

Action	Pilot Signal	Thresholds	Hysteresis band	Protection Output
Charge	SOC, I_{ref}	SOC > 1 & I_{ref} < 0 (charge)	0,01 pu SOC	[0, 1]
Discharge	SOC, I_{ref}	SOC <$SOC_{minimum}$ & I > 0 (discharge)	0,01 pu SOC	[0, 1]
Charge/Discharge	Temperature	360° C	10 °C	[0, 1]
Charge	Temperature, SOC	T_MAX= f(SOC)	10 °C	[0, 1]

Table 2. Protections Table

Moreover two limitation thresholds are present. The first one has to reduce the reference current whenever the, during a charge, the SOC is above 0.8 pu; while the second reduces the current if the temperature, during a discharge, reaches 340 °C.

Action	Pilot Signal	Thresholds	Hysteresis band	Protection Output
Charge	SOC	0.8 pu	0.1 pu SOC	Max current 2 → 0.5 pu
Discharge	Temperature	340 °C	10 °C	Max current 2 → 0.5 pu

Table 3. Limitation Table

4. Power plant layout and controllers

As foretold, the idea is to control the battery charging and discharging in order to control the whole plant output at the Point of Common Coupling (PCC). An overview of the layout

of the park is shown Fig. 20, the four 2 MW wind turbines are identified by the blocks on the right side of the picture while the battery is located in the central block.
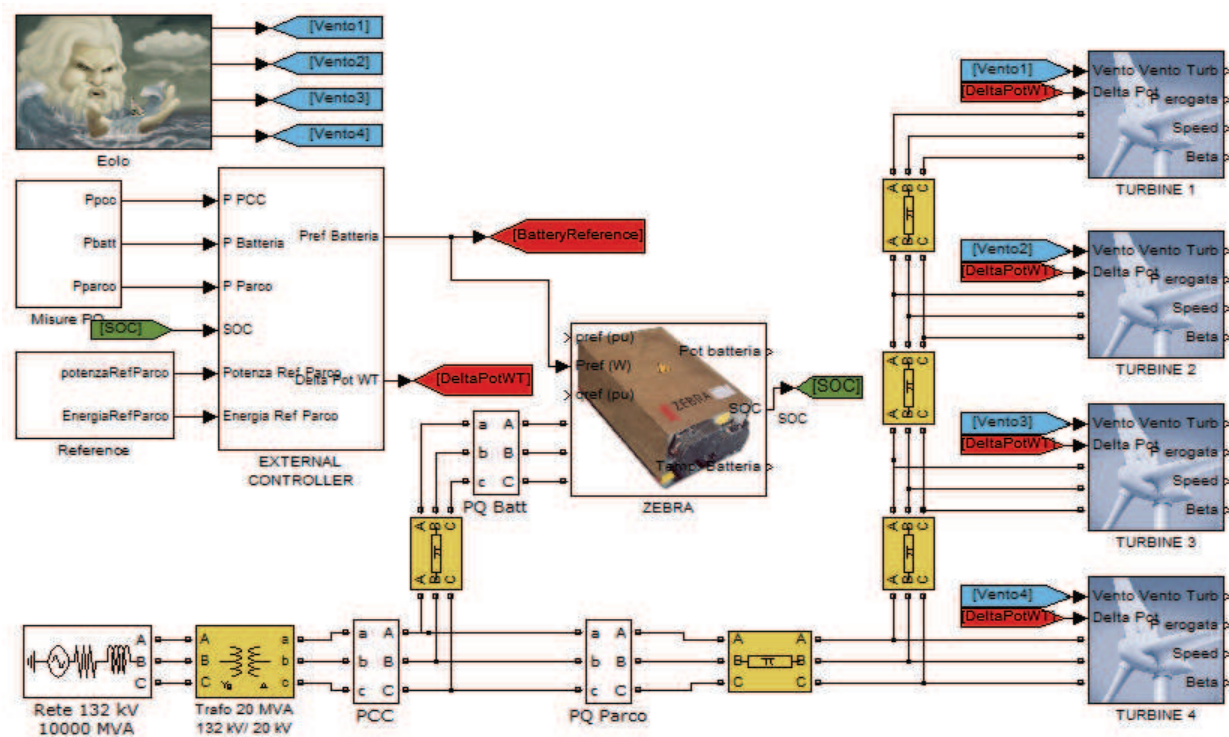

Fig. 20. Power plant layout

4.1 External battery controller

The external battery controller sets the reference power that the storage system has to accomplish. The controller, shown in Fig. 21, is equipped with a PI regulator and is sensible to the error between the power produced by all the wind turbines and the expected reference power. Moreover it is present in the control loop another contribution sensible to the SOC level of the battery (Yoshimoto et al., 2006). This control reduces or increases the battery reference power with the purpose to keep the SOC in an adequate range so that storage is always available.
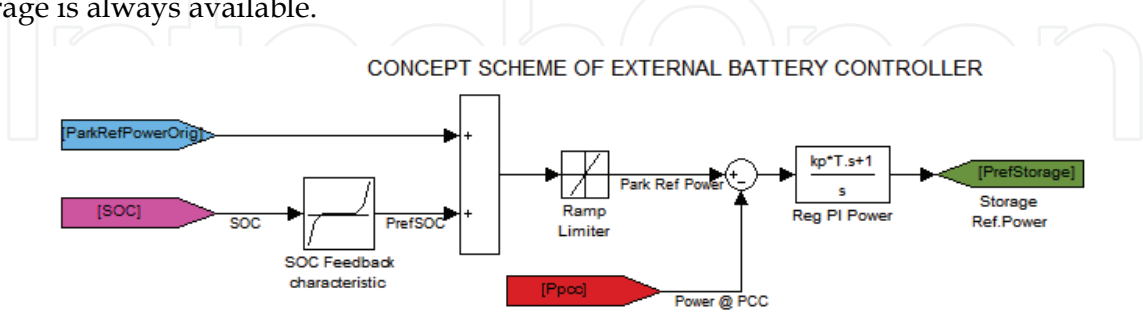

Fig. 21. Block diagram of the battery external controller

4.2 External wind turbine controller

The external wind turbine controller, shown in Fig. 22, forces the turbines to reduce their output, by means of a signal, generated by a PI controller sensible to the difference between

reference power and the power flowing at the PCC, which overrides the one generated by maximum power tracking curve. In fact, whenever there is the mandatory order from the Distribution System Operator to grant zero power transit at the PCC and the battery is not able to store the whole energy produced by the turbines, in order to avoid the complete shut down of the turbines, they can be forced to reduce their output. This situation can happen obviously if the storage is full, but also if it is above the threshold that reduces the charge intensity (i.e. SOC 0.8) and thus the battery is able to store just a fraction of wind production.
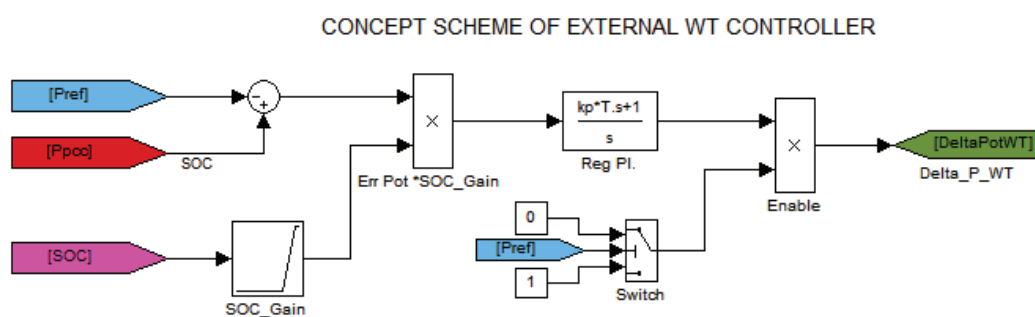

Fig. 22. Block diagram of the external wind turbine controller

5. Simulations & scenarios analyzed

The behaviours of the stand alone models are firstly tested. Thus the dynamic response of the wind turbine is tested by a sequence of wind steps starting from the cut-in speed (3 m/s) to the cut-out speed (25 m/s). The storage is tested by means of a sequence of both charge/discharge actions, with different magnitudes.

After that the models are coupled and two scenarios are studied: the first one regards the levelling of the overall wind park output in order to have a smoother power output at the PCC, the second one foresees the task to grant no power transit at the PCC for a certain time because of DSO request.

In order to perform these simulations it is assumed that the forecasted power output of the park is correct, that means that each ten minutes a reference power, which depends on the mean wind speed, is sent to the plants. It is clear that at each time step the wind turbines will not produce the forecasted power because of the turbulence. The main task is hence to smooth the fast fluctuation induced in the wind by the local terrain roughness.

5.1 Models testing: wind turbine

First of all the turbine model is tested by means of a series of wind steps, shown in the first diagram of Fig. 23 along with the pitch angle curve. The output power can be seen in the second diagram, while the rotational speed in the latter one. As long as the wind speed increases so does the rotational speed and therefore the output power. Once the wind reaches the nominal value (12 m/s) the power does not go above the nominal power (2 MW) and at each wind step the pitch controller keeps under control the rotational speed (1 pu) by increasing the pitch angle.

Fig. 24 offers an overview of the aero dynamical behaviour of the machine. The first diagram shows the increase of wind power with the increase of wind speed and the portion produced by the machine.
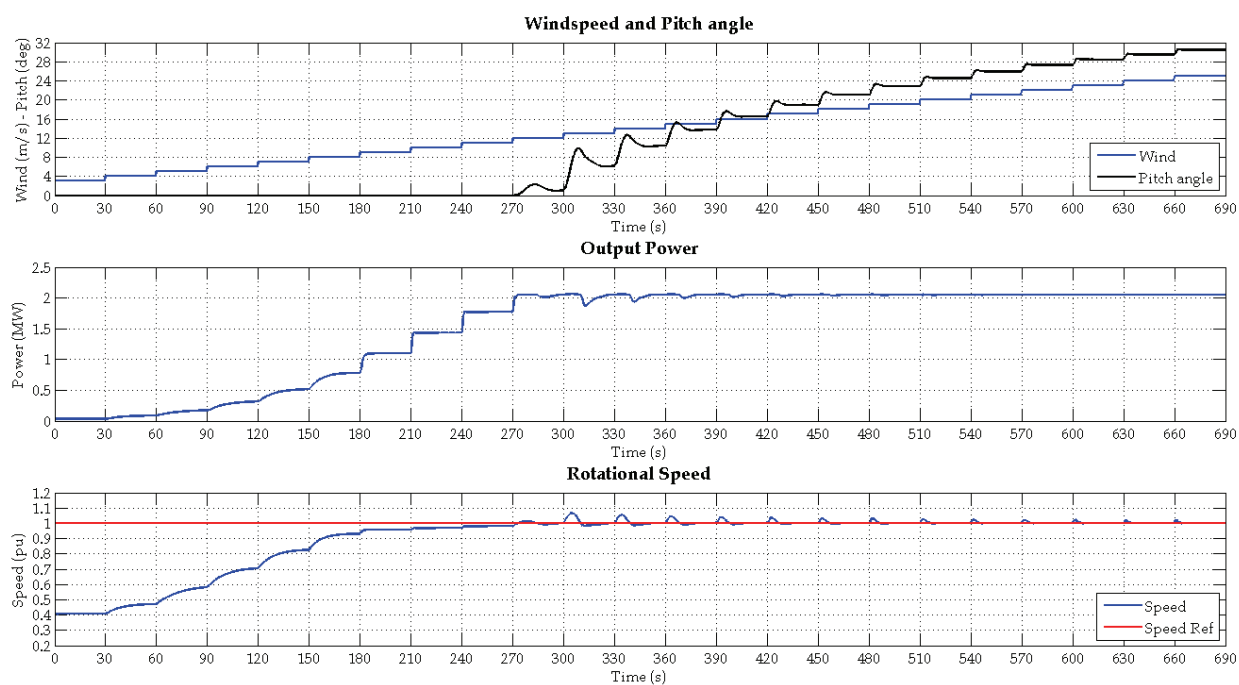
Fig. 23. Wind speed and pitch angle; Output power; Rotational speed
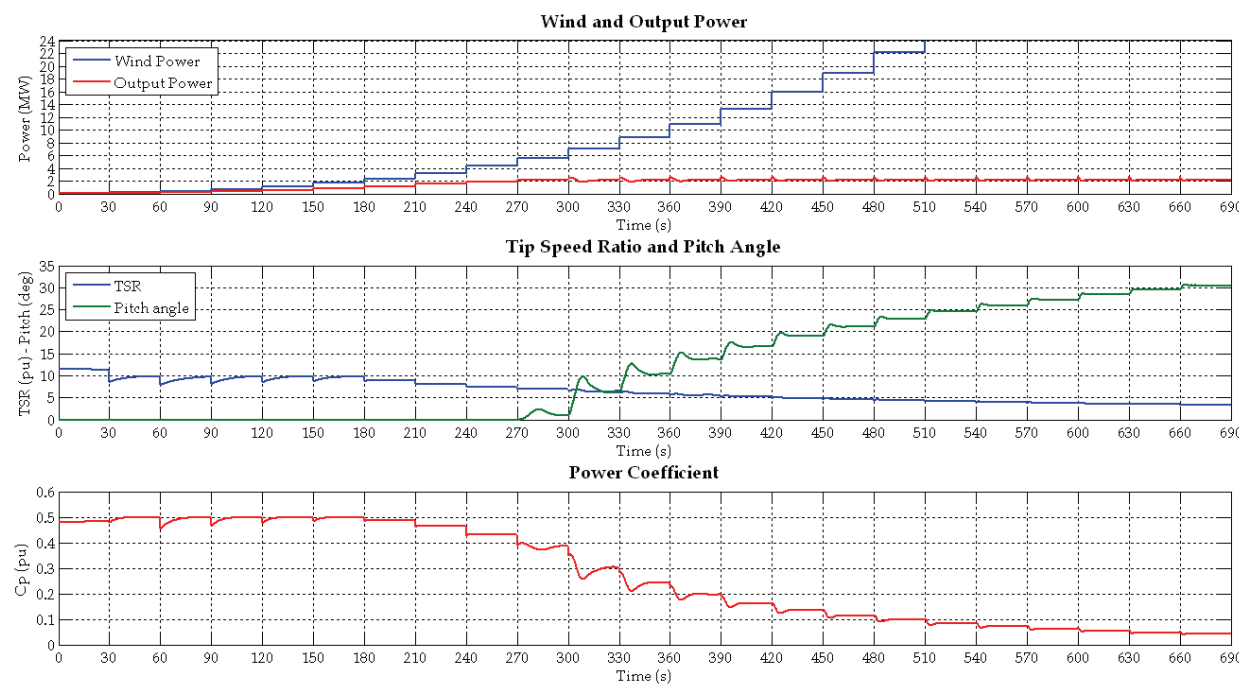

Fig. 24. Wind and output power; Tip speed ratio and pitch angle; Power coefficient

Because all the components of the machine are rated for 2 MW it is clear that all the amount of power present in strong winds cannot be harvested. The second diagram shows the Tip Speed Ratio (TSR or lambda), i.e. the ratio between the peripheral speed of the blades and the wind speed, and the pitch angle. As explained previously it is role of the MPT control to tune the rotational speed in order to pursue the optimal TSR (equal to 10 for the aerodynamic characteristic implemented in this turbine model) for light winds. As the wind

starts blowing stronger and the rotational speed reaches the limit (1 pu), the TSR is reduced contributing to the reduction of the power coefficient (cp, shown in the third diagram). The reduction of the TSR alone (see Fig. 8), however, is not enough to reduce the cp and, hence, it is necessary also to pitch the blades in order to reduce the lift of the blades.

The next step is to analyze the response of the four wind turbines, each fed by its own wind profile. Fig. 25 reports the simulation results for a 2-hours window simulation.
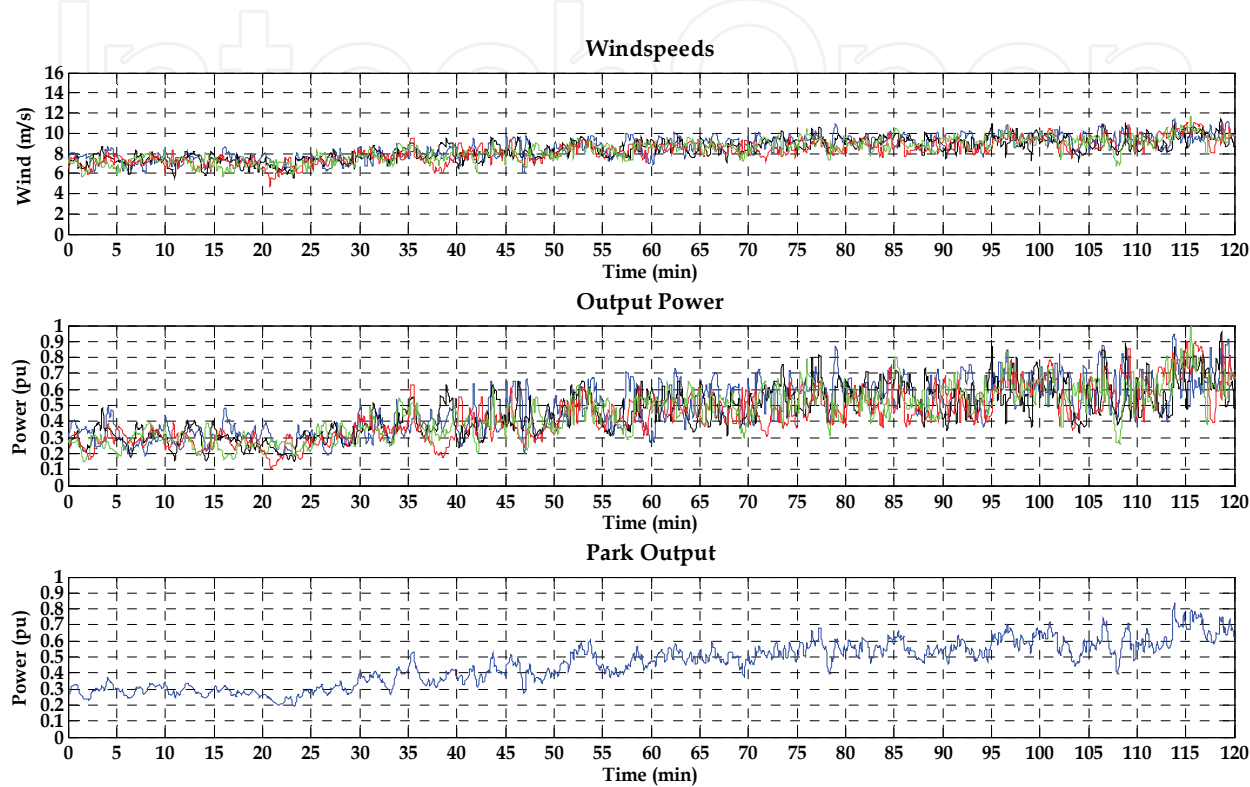

Fig. 25. Wind profiles; Turbines output; Park total output

The first diagram shows the wind profiles while the second one reports the respective power output in per unit on machine base (2 MW). The park output can be seen on the third diagram, in per unit again but on park base (8 MW). The overall power output certainly benefits from the mutual compensation of the turbines, that is due to the fact that one turbine can see a wind gust that, not necessarily, is seen by the others. The park output profiles, hence, improves with the increase of the machine number, however it is still quite turbulent. The measure of the power turbulence intensity, defined, similarly to the wind turbulence, as the ratio between the standard deviation and the average power in a 10-minutes basis, is about 19% (equal to 0.38 MW) for the single turbines while it is reduced to 11% (equal to 0.88 MW) at the PCC for the 2-hours timeframe considered.

5.2 Models testing: Storage

The storage size is 2.5 MW – 2 MWh and is chosen in order to compensate ± 3 times the PCC "power turbulence" intensity. The initial conditions are 60% SOC and 290 °C. Firstly a charge-discharge cycle at nominal power is performed followed by a more intense and shorter cycle at two time nominal power. The results are reported in Fig. 26, the first diagram shows the reference power that the battery is supposed to supply and the power

that can be provided. At the 19th minute the SOC level reaches 0.8 and that triggers the limitation in the charge action. The power that can be stored is reduced by half. The battery voltage is higher than the open circuit because the current has to flow inside the battery. At the 30th minute the charge is stopped and a discharge is required, the battery inverter thus sets a lower voltage in order to make the current flowing outside the battery. The controller has to progressively reduce the voltage in order to provide the required power, this because the lower is the SOC the higher gets the battery resistance (see Fig. 17).
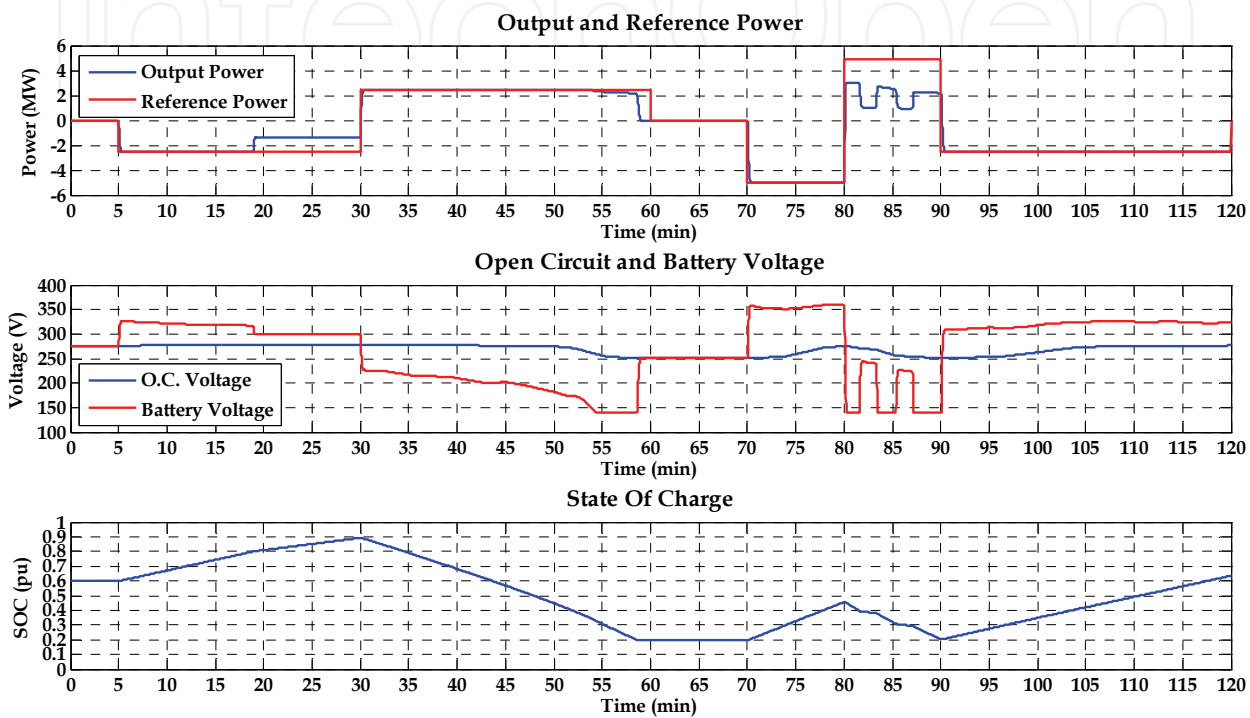

Fig. 26. Output and reference powers; Open circuit and battery voltage, SOC

When the SOC reaches 0.2 (58th minute) the minimum SOC protection stops the discharge. Afterward a more intense charge is required and successfully performed. At the 80th minute a deeper discharge is requested and the battery controller has to reduce the intensity several times due to the intervention of the thermal protection, as can be better appreciated in the Fig. 27. In the second diagram, in fact, at the 82nd minute the temperature reaches 340 °C that is the maximum allowed value. The power is hence reduced and as a result the joule losses drop (blue curve first diagram) and the thermal power removed by the fans (red curve) determines the reduction of the temperature. At the 90th minute the discharge action is terminated and a charge at nominal power is performed until the end of the simulation. In this last timeframe, the first diagram of Fig. 27 shows a sequence of turn on/off of the cooling fan (red curve) triggered by the thermal control system. The increase of the SOC, in fact, determines a reduction of the maximum allowed temperature.

5.3 Smoothing action

In this scenario is analyzed the coupling of the storage system with the wind farm. The mission of the battery is to smooth the wind farm output and the results are depicted in Fig. 28.
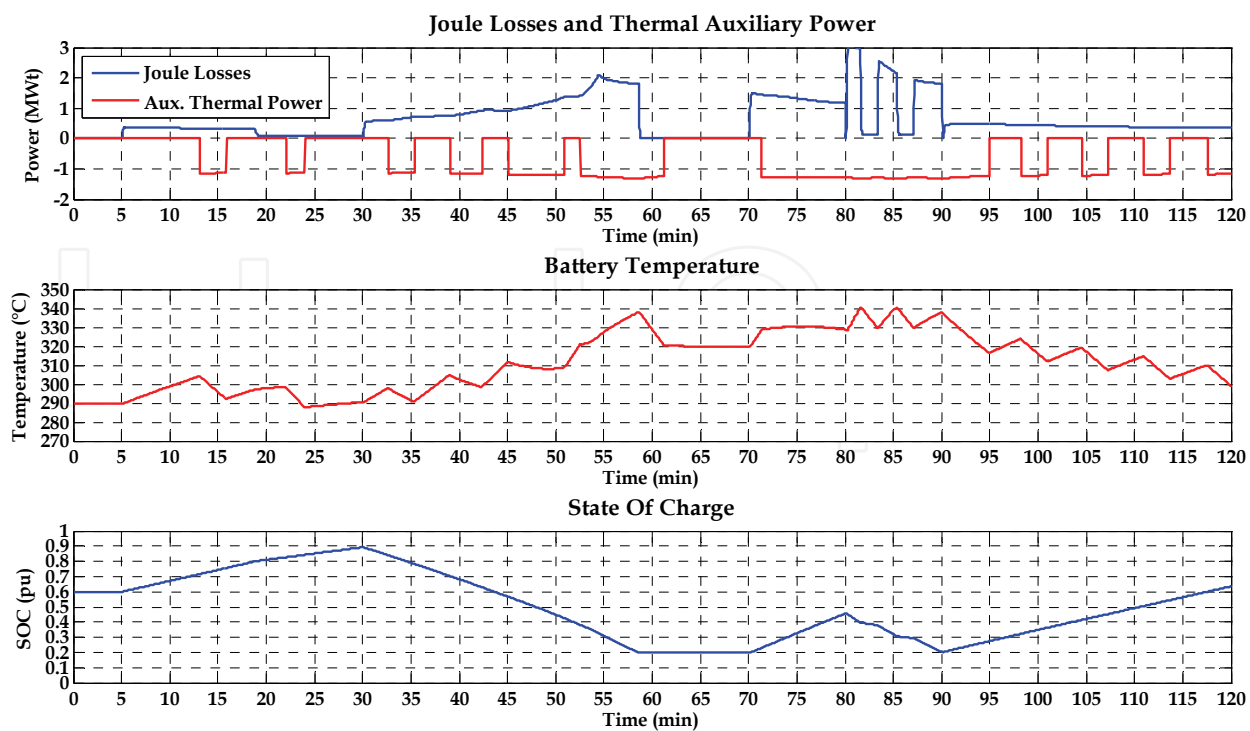
Joule Losses and Thermal Auxiliary Power

Battery Temperature

State Of Charge

Fig. 27. Joule losses and auxiliary thermal power; Cell temperature; SOC

Single Turbine Outputs
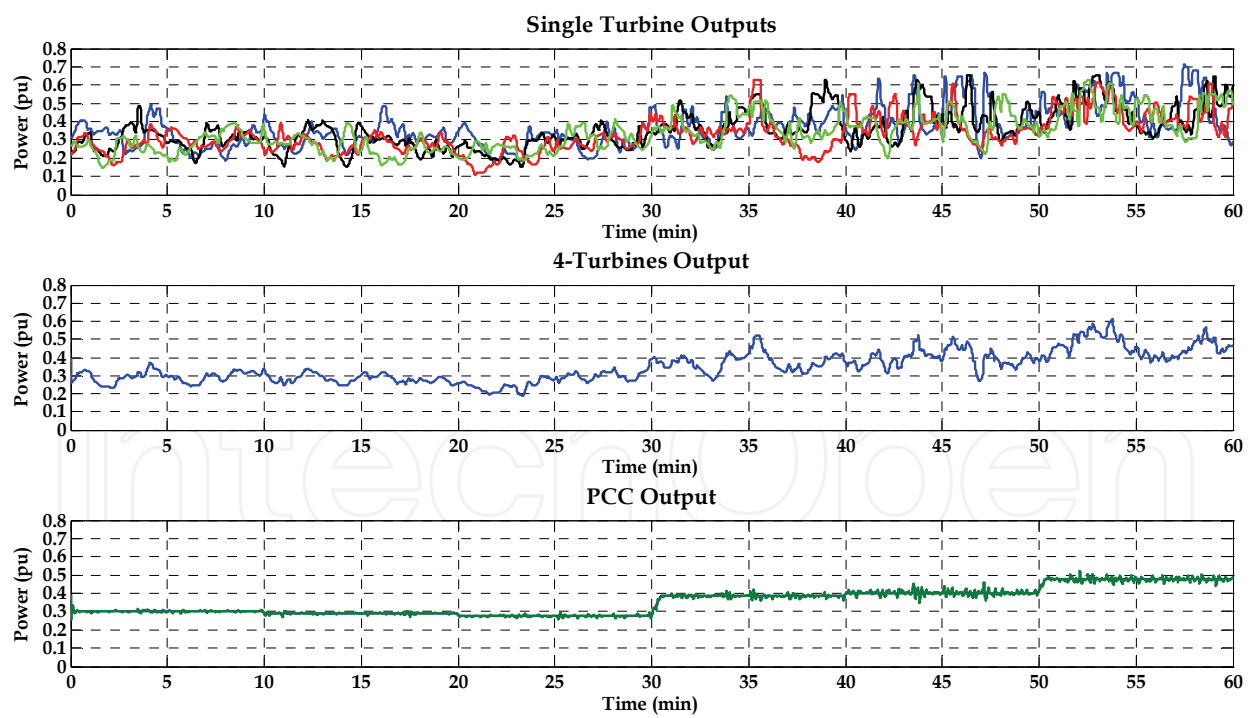

4-Turbines Output

PCC Output

Fig. 28. Single turbine outputs; 4-Turbines overall output; PCC output

The different turbine outputs are reported in the first diagram, while the overall wind production is depicted in the second diagram. The output power at the PCC, shown in the third diagram, presents a much smoother profile due to the compensation action of the battery. The storage system in fact, controlled by the reference set point sent by the external

controller, by the means of charge/discharge cycles is able to grant the expected reference power. Thus the wind turbulence is compensated by the storage. The "power turbulence" intensity, whose value is 11% for the power measured at the PCC, drops below the 3% for the 2-hours timeframe considered. The benefit of the storage is thus proved, however a warning must be raised concerning the stress that these charging/discharging cycles can have on the battery lifetime.

Fig. 29 offers an overview of the main storage variables: the power profile required and the one realized are shown in the first diagram, while the voltages are reported in the second one. The SOC is slightly decreasing because the battery has a non-null internal resistance and thus all these charge/discharge cycles deplete energy. The temperature instead is quite constant, meaning that the joule losses are matching the battery natural cooling.
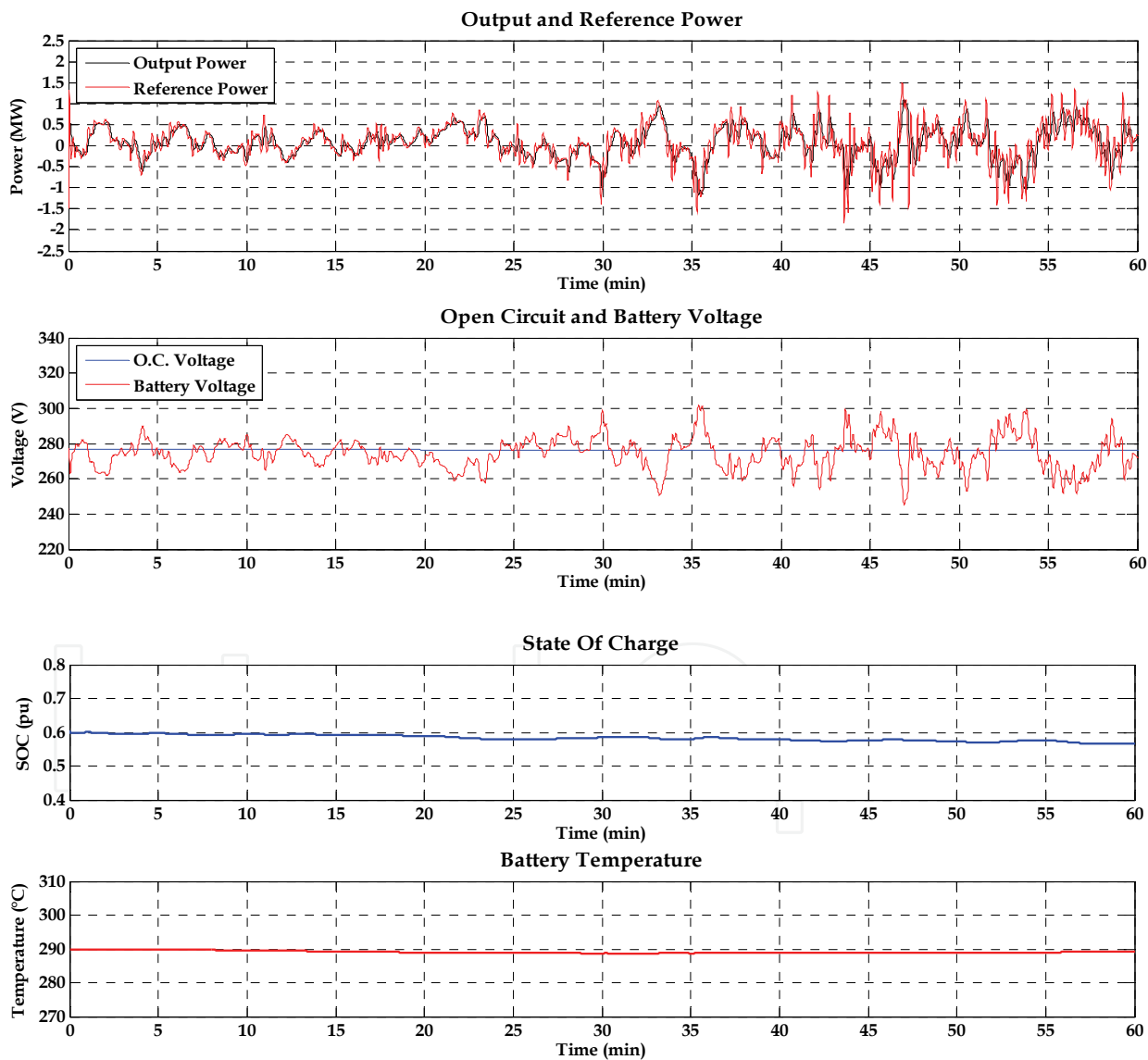

Fig. 29. Output and reference powers; O.C. and battery voltage; SOC; Cell temperature

5.4 Zero power transit at the PCC

In this last scenario the combined control of wind turbines and storage system is envisaged. It is supposed that the DSO requires no power transit at the PCC for half an hour, due for instance to congestions of the medium voltage network.

The third diagram of Fig. 30 reports the results for the power transit at the PCC: at the 2nd minute the battery begins to store the turbines' output in order to grant no power transit. Meanwhile the SOC, shown in Fig. 31, increases and when it reaches 0.8 (17th minute) the battery control system reduces the charging current and thus the power that the battery can store, because such an intensive charge cannot be born. The first diagram of Fig. 31 reports the actual level that the battery is allowed to manage and the request from the external battery controller that is trying to grant zero transit at the PCC. At this point the external controller of the turbines is enabled (see Fig. 22) and, by overriding the MPT controller, forces them to reduce their output.
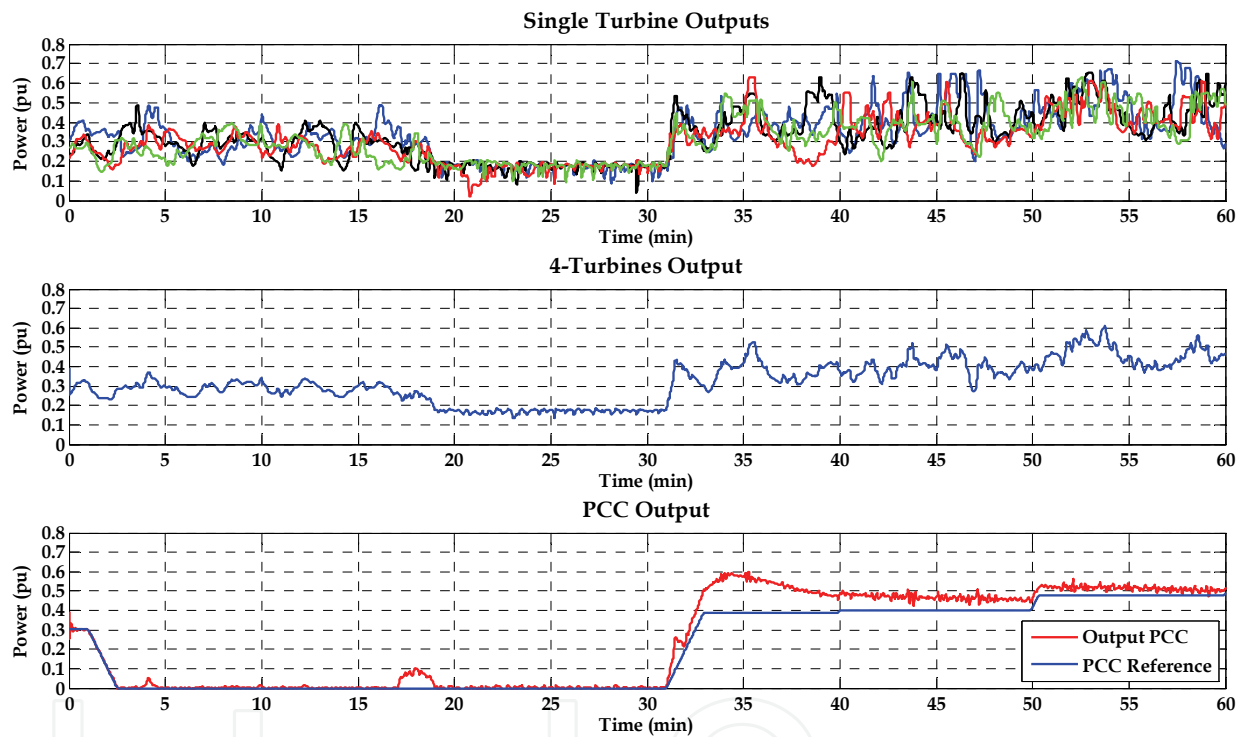

Fig. 30. Single turbine outputs; 4-Turbines overall output; PCC output and reference

This signal forces the reference power to a value that implies the acceleration of the turbines rotor, due to the unbalance between the mechanical torque (the accelerating one) and the electromagnetic torque of the generator (the braking one). The pitch control begins to increase the blade pitch angle to reduce the aero-dynamic efficiency and thus to contrast the rotor speed deviation. The wind turbine dynamics can be appreciated in Fig. 32 and Fig. 33.

When the DSO allows again power transit (31st minute) the MPT control of the turbines is fully restored and hence the turbines produce again the maximum power. The third diagram of Fig. 30 highlights an extra power production compared to the one that was programmed (blue line). This is due to the SOC feedback action of the battery external controller that forces the storage to release this amount of energy in order to take the SOC level far from the maximum level (see third diagram Fig. 31). As foretold this SOC feedback is needed to keep the battery within a reasonable range of values to avoid the block of the battery.
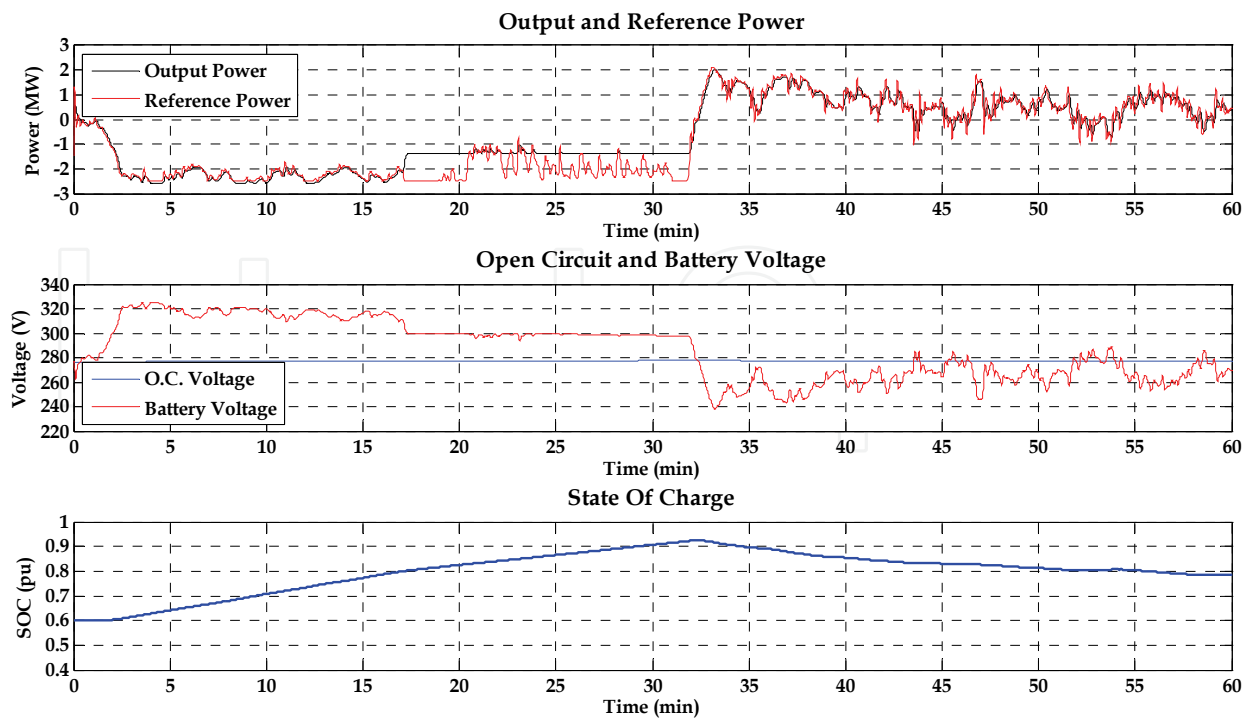
Output and Reference Power

Open Circuit and Battery Voltage

State Of Charge

Fig. 31. Output and reference powers; Open circuit and battery voltage; SOC

Windspeed and Pitch angle

Reference and Output Power
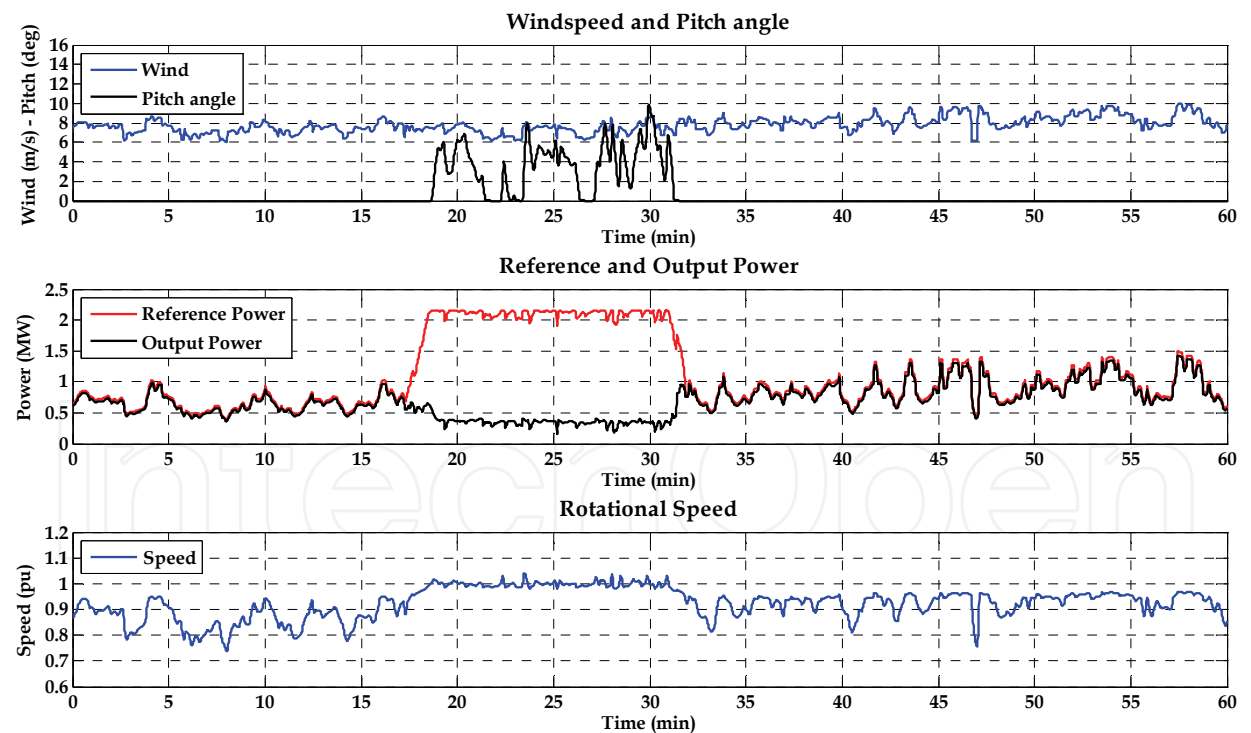
Rotational Speed

Fig. 32. Wind speed and pitch angle; Reference and output power; Rotational speed

It is interesting to analyze, in Fig. 32 and Fig. 33, the reduction of power in the turbines by the MPT override signal. This analysis can also help to better comprehend the wind turbine function. The power output reduction, in fact, is not realized by acting on the blades pitch angle but by the reduction of the reference power that the generator has to produce. The

consequent torques unbalance causes the over speed which is counteracted by the pitch controller. The reduction in the rotor efficiency, and hence the reduction of the power coefficient, is not realized by the blade pitching alone but also by the fact that the turbine is going to work with a Tip Speed Ratio well above the optimal one (second diagram Fig. 33). These two factors both contribute to reduce the power coefficient, whose behaviour is depicted in the third diagram.

When the turbine is allowed to extract again the maximum power, the MPT control, by setting the appropriate electromagnetic torque, takes the turbine rotational speed in the range that determines the optimal TSR. Obviously this happens because the wind is blowing between 6 and 9 m/s, thus there is the interest to harvest all the energy available in the wind. If the wind had blown stronger, the MPT controller would not have taken the turbine in the working point that determines the optimal TSR (see Fig. 24).
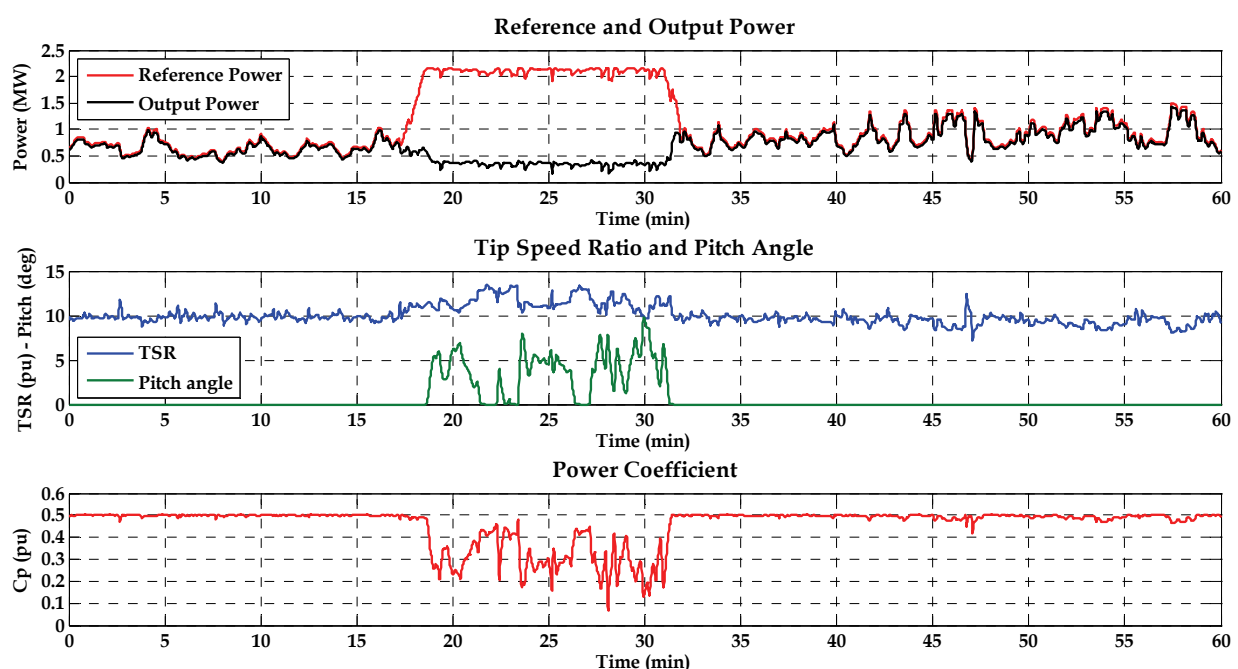

Fig. 33. Reference and output power; TSR and pitch angle; Power coefficient

6. Conclusions

The chapter focused on the development of models of wind turbines and storage systems, in Matlab-Simulink environment, for implementing integrated control strategies of the whole resulting system in order to describe the benefits that storage can provide.

A deep characterization of the wind profiles has been performed. The 2 MW turbine model was described from an electromechanical perspective, thus it provided: an analysis of the aerodynamic behaviour of the rotor including the pitch control system, the shaft dynamic and the maximum power tracking characteristic.

The storage model has been characterized from both the electrochemical and the thermal perspective. All the dynamics were built in the equivalent cell and the desired size of the battery (2.5 MW - 2 MWh) was obtained by multiplying the cell parameters for the number of series/parallel elements. The model presents a general validity and for this study has been tuned on the specifics of Na-NiCl$_2$ chemistry.

The control strategies analyzed had aimed at setting the battery charging and discharging phases in order to control the whole plant output.

The dynamics of the stand-alone models were studied by means of specific tasks: responses to wind steps and charge/discharge cycles at different intensity. Afterward the models have been coupled and two scenario were analyzed: the first one regarded the possibility to smooth the wind park turbulent output by charge/discharge control of the battery; the second one analyzed the possibility to control the storage to collect the power produced by the wind turbine in case of order by the DSO to reduce or to have zero power output at PCC and proved the possibility to reduce the wind farm output, without any turbine disconnection, in case of need.

It was thus highlighted how the storage system could grant benefits in term of controllability of the wind park output. However, the rigid power control, whose aim was to pursue a perfectly smoothed output, proved to be very stressful for the storage, threatening the battery lifetime. Nevertheless this control proved good performance in the zero transit scenario.
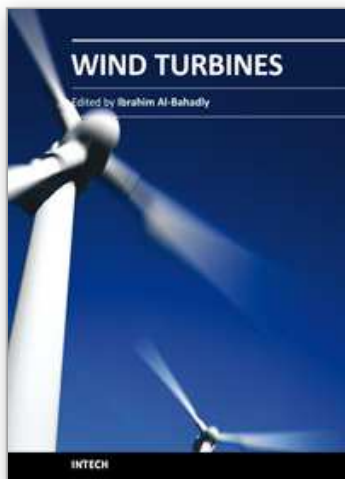
Further studies will regard the validation of the battery model, in order to insert proper values for the time constants and will envisage other control strategies as that sensible to an energy reference signal instead of the power one.

7. References

Thomas, R.J. (2009). Putting an action plan in place, *Power and Energy Magazine, IEEE*, vol. 7, no. 4, pp. 26-31, , July-Aug. 2009

Neural, A.; Kogan, V.I. & Schafer C.M. (2008). Load Leveling Reduces T&D Line Losses, *Power Delivery, IEEE Transactions on*, vol. 23, no. 4, pp. 2168–2173, Oct. 2008

Grillo, S.; Marinelli, M.; Pasca, E.; Petretto, G. & Silvestro, F. (2009). Characterization of Wind and Solar generation and their influence on distribution network performances, *Universities Power Engineering Conference (UPEC), 2009 Proceedings of the 44th International*, pp.1-6, 1-4 Sept. 2009, Glasgow

Fioravanti, R.; Vu, K.; Vu & Stadlin, W. (2008). Large scale solution, *Power and Energy Magazine, IEEE*, vol. 7, no. 4, pp. 48-57, July-Aug. 2009

Oudalov, A.; Chartouni, D.; Ohler, C. & Linhofer, G. (2006). Value Analysis of Battery Energy Storage Applications in Power Systems, *Power Systems Conference and Exposition, 2006. PSCE '06. 2006 IEEE PES*, pp.2206-2211, Oct. 29 2006-Nov. 1 2006

Di Rosa, D.; Fastelli, I.; Gigliucci, G.; Grillo, S.; Marinelli, M.; Massucco, S. & Silvestro, F. (2010). Generation and battery modelling and integrated control strategies for a better acceptance of intermittent renewable energy sources in the electric distribution system, *CIRED Workshop.* 7-8 June 2010, Lyon

Ackermann, T. et al. (2005). *Wind Power in Power Systems*, John Wiley and Sons Ltd, ISBN: 0470855088, New York

Marinelli, M.; Morini, A.; Pitto, A. & Silvestro, F. (2008). Modeling of doubly fed induction generator (DFIG) equipped wind turbine for dynamic studies, *Universities Power Engineering Conference, 2008. UPEC 2008. 43rd International*, pp. 1-6, 1-4 Sept. 2008, Padova

Achilles, S. & Pöller, M. (2004). Direct Drive Synchronous Machine Models for Stability Assessment of Wind Farm, *DIgSILENT Publications,* 2004

Sørensen, P.; Hansen, A.; Janosi, L.; Bech, J. & Bak-Jensen, B. (2001). Simulation of interaction between wind farm and power system. *Risø-R-1281, Risø National Laboratory, Roskilde*. December 2001

Hansen, A.; Iov, F.; Sørensen, P.; Cutululis, N.; Jauch, C. & Blaabjerg, F. (2007). Dynamic wind turbine models in power system simulation tool DIgSILENT. *Risø-R-1400 ed.2, Risø National Laboratory, Roskilde*. August 2007

Akhmatov V. (2003). Analysis of dynamic behaviour of dynamic power systems with large amount of wind power. *PhD Thesis, Orsted DTU*, 2003

Chen, M. & Rincon Mora, A. (2006). Accurate Electrical Battery Model Capable of Predicting Runtime and I–V Performance, *Energy Conversion, IEEE Transactions on*, vol. 21, no. 2

Bossi, C.; Buonarota, A. & Micolano, E. (2005). Risultati delle prove di laboratorio condotte su accumulatori avanzati. *Ricerca di Sistema, Technical Report*, Milano, 2005

Yoshimoto, K.; Nanahara, T.; Koshimizu, G. & Uchida, Y. (2006). New Control Method for Regulating State-of-Charge of a Battery in Hybrid Wind Power/Battery Energy Storage System, *Power Systems Conference and Exposition, 2006. PSCE '06. 2006 IEEE PES*, pp. 1244-1251, Oct. 29 2006-Nov. 1 2006

Wind Turbines

Edited by Dr. Ibrahim Al-Bahadly

The area of wind energy is a rapidly evolving field and an intensive research and development has taken place in the last few years. Therefore, this book aims to provide an up-to-date comprehensive overview of the current status in the field to the research community. The research works presented in this book are divided into three main groups. The first group deals with the different types and design of the wind mills aiming for efficient, reliable and cost effective solutions. The second group deals with works tackling the use of different types of generators for wind energy. The third group is focusing on improvement in the area of control. Each chapter of the book offers detailed information on the related area of its research with the main objectives of the works carried out as well as providing a comprehensive list of references which should provide a rich platform of research to the field.

How to reference

In order to correctly reference this scholarly work, feel free to copy and paste the following:

Samuele Grillo, Mattia Marinelli and Federico Silvestro (2011). Wind Turbines Integration with Storage Devices: Modelling and Control Strategies, Wind Turbines, Dr. Ibrahim Al-Bahadly (Ed.), ISBN: 978-953-307-221-0, InTech, Available from: http://www.intechopen.com/books/wind-turbines/wind-turbines-integration-with-storage-devices-modelling-and-control-strategies

INTECH

open science | open minds